Volume 10, Number 3, 2017. pp. 165-172

Jordan Journal of Physics

ARTICLE

Electromagnetic Transmission from a Dielectric Loaded Resistive Cylindrical Pipe

M. S. Bawa'aneh, A. M. Al-Khateeb and **N. Laham**

Department of Physics, Yarmouk University, Irbid, Jordan.

Received on: 24/5/2017; Accepted on: 9/8/2017

Abstract: We obtained analytically closed form expressions for longitudinal electric impedance and transmission coefficient of a dielectric loaded resistive cylindrical pipe of finite thickness. These expressions are valid for an axial current in a form of a point source moving parallel to the pipe axis with an offset a. The resistive–wall impedance and the transmission coefficient have been numerically visualized for some representative machine parameters. For wall thicknesses less than the skin penetration depth, the wall becomes transparent for the excited electromagnetic fields. Very good shielding for standard operation can be achieved by thin metallic walls of thicknesses of the order of few skin penetration depths. Effects of the dielectric constant and thickness on the transmission coefficient are found to be negligibly small, while the presence of the dielectric leads to a suppression of resistive-wall impedance for large thicknesses of the dielectric layer.
Keywords: Cylindrical pipe, Electrical impedance, Transmission coefficient, Wave guides.

Introduction

Axial currents, like a beam of charged particles or an RF-source, may excite electromagnetic fields in its environment and periodic excitations can occur depending on the coupling of the beam to its environment at a particular frequency.

For pipe walls that are not perfectly conducting, electromagnetic fields excited by the beam penetrate partially into the pipe wall with a penetration depth given by the skin depth $\delta_s(\omega)$. Image currents induced in the wall lead to heating when the wall conductivity is not infinite. In the literature of electric impedances [1, 2], one finds different expressions for the corresponding resistive–wall impedance with different ranges of validity. When the skin depth is larger than the wall thickness, the beam induces electromagnetic fields that can penetrate through the wall. In such cases, the impedance depends on the structures outside the pipe. In this situation, in addition to the impedance, detailed calculations of the shielding effectiveness of the pipe are necessary in order to estimate the currents that could be induced in hardware components behind the pipe.

The well known ability of a thin layer of thickness d (less than the skin depth δ_s) to shield electromagnetic fields produced by a particle beam was considered in Ref. [3]. Because of the relevance of the issue for the design of high-current ring machines, it is important to have closed form expressions for the resistive wall impedance and for the shielding effectiveness covering the relevant range of frequencies, beam energies and wall thicknesses. Krinski et al. [4] derived asymptotic formulae for the impedance of a cylindrical metal tube of a specific radius, length and conductivity attached at each end to perfect conductors of semi-infinite length and computed the short-range wake field. Metral et al. [5] derived a formula for the resistive wall impedances of an infinitely long cylindrical beam pipe. They found that the resistive impedance is about two orders of magnitude

Corresponding Author: M. S. Bawa'aneh **Email**: msbawaaneh@yu.edu.jo

lower at this frequency, which is explained by the fact that the skin depth is much larger than the beam pipe radius. Zhilichev [7] derived an analytical form for the impedance of short conductors in the form of a convergent series and applied it to the calculation of the impedance of a resistive cylinder between two superconductors. Biancacci et al. [8] studied the effect of different material conductivities, finite length and particle beam velocity on the coupling impedance of azimuthally symmetric cavities of finite length loaded with a toroidal slab of lossy dielectric using the method of mode matching technique for an azimuthally uniform structure of finite length.

In the present work, we consider the problem of the interaction between a dielectric-lined resistive cylindrical pipe and a point source moving off-axis with an offset a (an infinitesimally thin ring with radius a). Such a scheme was used in investigating dielectric wake-field accelerators, in which charged particle beams excite electromagnetic wake fields known as Čerenkov radiation [9, 10, 11]. In the frequency domain, we are interested in evaluating the excited electromagnetic fields in such a dielectric-lined cylindrical pipe and then in finding the corresponding resistive-wall impedance and transmission coefficient for our problem.

The paper is organized as follows. In the next section, we present the model equations for the pipe structure under consideration. Then, in the following two sections, we use the exact field matching technique to calculate the excited electromagnetic fields and the corresponding longitudinal electric impedance and transmission coefficient. In the last section, the analytical expressions for resistive–wall impedance and transmission will be numerically visualized and main conclusions will be presented.

Model Equations

The general wave equations satisfied by the electric and magnetic fields $\vec{E}$ and $\vec{B}$ in a linear medium of conductivity S, permittivity f and permeability μ are obtained from Faraday's and Ampere's laws [12, 13, 14]; namely,

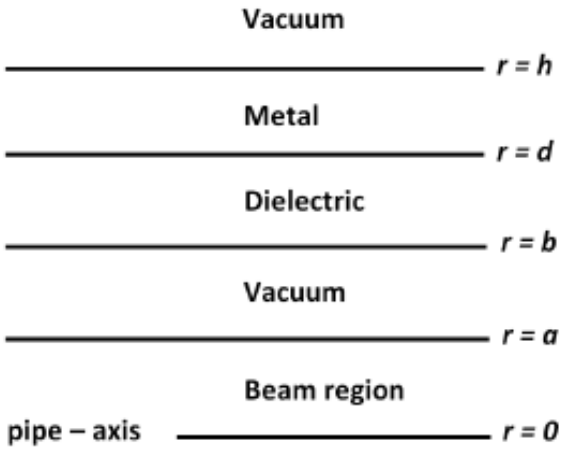

FIG. 1. Schematic of the problem geometry.

$$\nabla^2\vec{B}(\vec{r},t) - \mu\epsilon\frac{\partial^2\vec{B}(\vec{r},t)}{\partial t^2} - \mu S\,\frac{\partial\vec{B}(\vec{r},t)}{\partial t} = -\mu\vec{\nabla}\times\vec{j}(\vec{r},t)\,, \tag{1}$$

$$\nabla^2\vec{E}(\vec{r},t) - \mu\epsilon\frac{\partial^2\vec{E}(\vec{r},t)}{\partial t^2} - \mu S\,\frac{\partial\vec{E}(\vec{r},t)}{\partial t} = \mu\frac{\partial\vec{j}(\vec{r},t)}{\partial t} + \frac{\vec{\nabla}\rho(\vec{r},t)}{\epsilon}\,, \tag{2}$$

where ρ and $\vec{j}$ are the beam charge and current densities, respectively, which obey the following continuity equation:

$$\frac{\partial\rho(\vec{r},t)}{\partial t} + \vec{\nabla}\cdot\vec{j}(\vec{r},t) = 0\,. \tag{3}$$

The axial current is modeled as a point charge q_0 moving down a cylindrical pipe with an offset a in the $\theta_0 = 0$ direction with a constant longitudinal velocity $\vec{v} = \beta_0 c\hat{z}$. In decomposing the corresponding charge and current densities in terms of multipole moments, the lowest monopole moment is:

$$\rho(\vec{r},t) = \frac{q_0}{2\pi a}\,\delta(a-r)\,\delta\left(z-\beta_0 ct\right)\,, \tag{4}$$

$$\vec{j}(\vec{r},t) = \frac{q_0}{2\pi a}\,\delta(a-r)\,\delta\left(z-\beta_0 ct\right)\,\beta_0 c\hat{z}\,. \tag{5}$$

This monopole source has an axially symmetric transverse charge distribution and it represents an infinitesimally thin ring with radius *a*. The beam is moving in a cylindrical pipe of radius *b*, enclosed from inside to outside, respectively, by a dielectric of thickness t_d and dielectric constant κ_d, a conducting layer of conductivity *S* and thickness t_c, then vacuum outside, as shown in Fig 1.

Time Fourier–transformed charge and current densities in Eqs. (4) and (5) are:

$$\rho(r,z,\omega) = \frac{q_0}{2\pi a\beta_0 c}\,\delta(a-r)\,e^{ik_z z}, \tag{6}$$

$$j(r,z,\omega) = \frac{q_0}{2\pi a}\,\delta(a-r)\,e^{ik_z z}\,, \tag{7}$$

where $\omega = k_z\beta_0 c$ has been used and k_z is the wave number in the direction of beam propagation.

Due to the symmetry of the source under consideration, only transverse magnetic (TM) cylindrical waveguide modes couple to the propagating beam such that $B_z = 0$. All other field components are obtained from $E_z(r, z, \omega)$ using Maxwell's equations, where $E_\theta(r, z, \omega)$ and $B_r(r, z, \omega)$ vanish identically because of the axial symmetry of the beam.

We assume normal mode solution for the time Fourier–transformed electric field such that $E_z(r, z, \omega) = E_z(r, \omega)e^{ik.z}$. This is in agreement with the source terms in Eqs. (6) and (7). Upon Fourier transforming Eq. (2) in time and making use of $\rho(r, z, \omega)$ and $j(r, z, \omega)$ of Eqs. (6) and (7), respectively, we obtain the following equations for the longitudinal electric field component E_z within each region of interest:

$$\left[\frac{d^2}{dr^2}+\frac{1}{r}\frac{d}{dr}-\sigma_0^2\right]E_z^{(1)}(r,\omega) = i\frac{q_0}{2\pi a}\frac{k_z}{\epsilon_0\gamma_0^2\beta_0 c}\,\delta(a-r)\,,\quad 0\le r\le a \tag{8}$$

$$\left[\frac{d^2}{dr^2}+\frac{1}{r}\frac{d}{dr}-\sigma_0^2\right]E_z^{(2)}(r,\omega) = 0\,,\qquad a\le r\le b \tag{9}$$

$$\left[\frac{d^2}{dr^2}+\frac{1}{r}\frac{d}{dr}-\sigma_d^2\right]E_z^{(3)}(r,\omega) = 0\,,\qquad b\le r\le d=b+t_d \tag{10}$$

$$\left[\frac{d^2}{dr^2}+\frac{1}{r}\frac{d}{dr}-\sigma_c^2\right]E_z^{(4)}(r,\omega) = 0\,,\qquad d\le r\le h=d+t_c \tag{11}$$

$$\left[\frac{d^2}{dr^2}+\frac{1}{r}\frac{d}{dr}-\sigma_0^2\right]E_z^{(5)}(r,\omega) = 0\,,\qquad h\le r<\infty \tag{12}$$

where the propagation wave numbers σ_0, σ_d and σ_c are given by the following expressions:

$$\sigma_0^2 = \frac{k_z^2}{\gamma_0^2}\,,\quad \sigma_d^2 = k_z^2\left(1-\beta_0^2\kappa_d\right)\,,\quad \sigma_c^2 = \sigma_0^2\left(1+i\frac{\omega\gamma_0^2\mu_0 S}{k_z^2}\right)\,,\quad \gamma_0^{-2} = 1-\beta_0^2\cdot \tag{13}$$

Since the structure under consideration supports only transverse magnetic modes due to azimuthal symmetry of the source, the electromagnetic field components $B_\theta(r, z, \omega)$ and $E_r(r, z, \omega)$ are non-vanishing and are needed for matching the solutions at the different interfaces involved in the problem. These fields are obtained from $E_z(r, z, \omega)$ via Maxwell equations as follows:

$$E_r(r,z,\omega) = -i\,\frac{k_z}{\sigma_\alpha^2}\,\frac{\partial E_z(r,z,\omega)}{\partial r}\,, \tag{14}$$

$$B_\theta(r,z,\omega) = \left(\frac{\beta}{c} + i\frac{\mu_0\beta c S}{\omega}\right)\,E_r(r,z,\omega) \tag{15}$$

where σ_α stands for σ_0, σ_d and σ_c.

Excited Electromagnetic Fields

In this section, we solve the wave equation for E_z in each region and then find the associated integration constants using exact field matching. For TM modes in azimuthally symmetric pipe structures, we only solve for the z–component of the electric field in the five regions involved in the problem. The general solution for the electric field E_z in each region is:

$$E_z(r,\omega) = \begin{cases} A_1 I_0(\sigma_0 r) & 0 \le r \le a \\ A_2 I_0(\sigma_0 r) + A_3 K_0(\sigma_0 r) & a \le r \le b \\ A_4 I_0(\sigma_d r) + A_5 K_0(\sigma_d r) & b \le r \le d = b + t_d \\ A_6 I_0(\sigma_c r) + A_7 K_0(\sigma_c r) & d \le r \le h = b + t_c \\ A_8 K_0(\sigma_0 r) & h \le r < \infty\,, \end{cases} \tag{16}$$

where I_0 and K_0 are the zero-order modified Bessel functions of first and second kinds, respectively. In addition to the finiteness of E_z as $r \to 0$ and $r \to \infty$, we still have eight arbitrary constants and therefore eight boundary conditions are needed. Integrating the differential equation for E_z from $r = a - \delta$ to $r = a + \delta$ for vanishingly small δ, we obtain the following boundary condition for the discontinuity of $\partial E_z/\partial r$ at $r = a$:

$$\left(E_z'^{\,r\ge a} - E_z'^{\,r\le a}\right)\Big|_{r=a} = i\frac{1}{\epsilon_0\gamma_0\beta c}\,\frac{q_0}{2\pi a} \equiv i q_0 f_0\,, \tag{17}$$

where E_z' is the derivative of E_z with respect to $\sigma_0 r$. We also use the continuity of E_z at $r = a$, the continuity of E_z and B_θ at $r = b$, $r = d$ and $r = h$. Applying the above mentioned eight boundary conditions, we obtain the following eight algebraic equations:

$$A_1 I_0(\sigma_0 a) = A_2 I_0(\sigma_0 a) + A_3 K_0(\sigma_0 a)\,, \tag{18}$$

$$A_2 I_1(\sigma_0 a) - A_3 K_1(\sigma_0 a) - A_1 I_1(\sigma_0 a) = i\frac{1}{\epsilon_0\gamma_0\beta c}\,\frac{q_0}{2\pi a} \equiv i\,q_0\,f_0\,, \tag{19}$$

$$A_2 I_0(\sigma_0 b) + A_3 K_0(\sigma_0 b) = A_4 I_0(\sigma_d b) + A_5 K_0(\sigma_d b)\,, \tag{20}$$

$$A_2 I_1(\sigma_0 b) - A_3 K_1(\sigma_0 b) = \eta_{\rm dv}\left[A_4 I_1(\sigma_d b) - A_5 K_1(\sigma_d b)\right]\,, \tag{21}$$

$$A_4 I_0(\sigma_d d) + A_5 K_0(\sigma_d d) = A_6 I_0(\sigma_c d) + A_7 K_0(\sigma_c d)\,, \tag{22}$$

$$A_4 I_1(\sigma_d d) - A_5 K_1(\sigma_d d) = \eta_{\rm cd}\left[A_6 I_1(\sigma_c d) - A_7 K_1(\sigma_c d)\right]\,, \tag{23}$$

$$A_6 I_0(\sigma_c h) + A_7 K_0(\sigma_c h) = A_8 K_0(\sigma_0 h)\,, \tag{24}$$

$$\eta_{\rm cv}\left[A_6 I_1(\sigma_c h) - A_7 K_1(\sigma_c h)\right] = -A_8 K_1(\sigma_0 h)\,, \tag{25}$$

where η_{cv}, η_{cd} and η_{dv} are defined as follows:

$$\eta_{\rm cv} = i\frac{\sigma_0}{\sigma_c}\,\frac{S - i\omega\epsilon_0}{\omega\epsilon_0}\,,\ \eta_{\rm cd} = i\frac{\sigma_d}{\sigma_c}\,\frac{S - i\omega\epsilon_0}{\omega\epsilon_0\kappa_d}\,,\ \eta_{\rm dv} = \frac{\kappa_d\sigma_0}{\sigma_d}\,. \tag{26}$$

The arbitrary constant A_1 needed for the determination of the longitudinal electric field inside the beam region and for the calculation of longitudinal impedance is obtained by simultaneously solving the system of Eqs. (18–25); namely,

$$E_z^{r\le a}(\vec{r},\omega) = -i\,\frac{Z_0 k_z I_0(\sigma_0 a) I_0(\sigma_0 r)\, e^{ik_z z}}{2\pi\gamma_0^2\beta_0}\left[\frac{f_1 f_3}{f_4}\,\frac{\alpha_{12}-\alpha_{22}}{\alpha_{11}\alpha_{22}-\alpha_{12}\alpha_{21}} - f_2 + \frac{K_0(\sigma_p a)}{I_0(\sigma_p a)}\right], \quad (27)$$

where the parameters in Eq. (27) are given by the following relations:

$$\alpha_{11} = \frac{K_0(\sigma_d d)}{I_0(\sigma_d d)} - \frac{f_5}{f_4}, \quad \alpha_{22} = \eta_{\mathrm{cd}}\left[\frac{K_1(\sigma_c d)}{I_1(\sigma_d d)} + \frac{f_7}{f_6}\frac{I_1(\sigma_c d)}{I_1(\sigma_d d)}\right] \quad (28)$$

$$\alpha_{12} = -\left[\frac{K_0(\sigma_c d)}{I_0(\sigma_d d)} - \frac{f_7}{f_6}\frac{I_0(\sigma_c d)}{I_0(\sigma_d d)}\right], \quad \alpha_{21} = -\left[\frac{f_5}{f_4} + \frac{K_1(\sigma_d d)}{I_1(\sigma_d d)}\right] \quad (29)$$

$$f_1 = \frac{K_0(\sigma_d b)}{I_0(\sigma_0 b)} - \frac{f_5}{f_4}\frac{I_0(\sigma_d b)}{I_0(\sigma_0 b)}, \quad f_2 = \frac{K_0(\sigma_0 b)}{I_0(\sigma_0 b)} - \frac{f_3}{f_4}\frac{I_0(\sigma_d b)}{I_0(\sigma_0 b)} \quad (30)$$

$$f_3 = \frac{K_1(\sigma_0 b)}{I_1(\sigma_0 b)} + \frac{K_0(\sigma_0 b)}{I_0(\sigma_0 b)}, \quad f_4 = \frac{I_0(\sigma_d b)}{I_0(\sigma_0 b)} - \eta_{\mathrm{dv}}\frac{I_1(\sigma_d b)}{I_1(\sigma_0 b)} \quad (31)$$

$$f_5 = \frac{K_0(\sigma_d b)}{I_0(\sigma_0 b)} + \eta_{\mathrm{dv}}\frac{K_1(\sigma_d b)}{I_1(\sigma_0 b)} \quad (32)$$

$$f_6 = \frac{I_0(\sigma_c h)}{K_0(\sigma_0 h)} + \eta_{\mathrm{cv}}\frac{I_1(\sigma_c h)}{K_1(\sigma_0 h)} \quad (33)$$

$$f_7 = \frac{K_0(\sigma_c h)}{K_0(\sigma_0 h)} - \eta_{\mathrm{cv}}\frac{K_1(\sigma_c h)}{K_1(\sigma_0 h)} \quad (34)$$

Longitudinal Impedance and Transmission

Longitudinal electric impedance will now be calculated as a volume integral over the beam current by assuming a circular accelerator of circumference L [1, 2]:

$$\begin{aligned} Z_{\parallel}^{(\mathrm{total})}(\omega,S) &= -\frac{1}{q_0^2}\int_{V_b} d^3r\,\vec{E}^{(r\le a)}(\vec{r},\omega)\cdot\vec{j}^{*}(\vec{r},\omega) \\ &= -\frac{1}{q_0^2}\int_0^L dz\int_0^{2\pi} d\theta\int_0^a dr\,r\,E_z^{(r\le a)}(\vec{r},\omega)\,j^{*}(\vec{r},\omega). \end{aligned} \quad (35)$$

Substituting for E_z and j results in the following expression for the electric impedance:

$$Z_{\parallel}^{(\mathrm{total})}(\omega,S) = i\,\frac{nZ_0 I_0^2(\sigma_0 a)}{\beta_0\gamma_0^2}\left[\frac{f_1 f_3}{f_4}\,\frac{\alpha_{12}-\alpha_{22}}{\alpha_{11}\alpha_{22}-\alpha_{12}\alpha_{21}} - f_2 + \frac{K_0(\sigma_0 a)}{I_0(\sigma_0 a)}\right], \quad (36)$$

where $Z_0 = 1/\varepsilon_0 c$ is the vacuum impedance and n denotes the harmonic number which is related to the ring radius R by the relation $n = k_z R$ [1, 2]. The resistive-wall part of the longitudinal electric impedance $Z_{||}^{(rw)}(\omega,S)$ is as follows:

$$Z_{\parallel}^{(\mathrm{rw})}(\omega,S) = Z_{\parallel}^{(\mathrm{total})}(\omega,S) - Z_{\parallel}^{(\mathrm{total})}(\omega,S\to\infty), \quad (37)$$

where $Z_{||}^{(rw)}(\omega,S\to\infty)$ accounts for the absence of resistivity and represents the space-charge part of the electric impedance.

The longitudinal transmission coefficient $\tau_{||}$ of the resistive cylindrical pipe is obtained as the ratio of the transmitted to incident field amplitudes [2] and can be written as follows:

$$\tau_{||} = \frac{(\alpha_{11} - \alpha_{21})\left[K_0(\sigma_c h) - \frac{f_7}{f_6} I_0(\sigma_c h)\right]}{\left(\frac{f_5}{f_4}(\alpha_{12} - \alpha_{22}) - (\alpha_{11}\alpha_{22} - \alpha_{12}\alpha_{21})\right) I_0(\sigma_d d) - (\alpha_{22} - \alpha_{12}) K_0(\sigma_d d)} . \quad (38)$$

Numerical Examples

We obtained analytically closed form expressions for longitudinal electric impedance and transmission coefficient of a resistive cylindrical pipe of a conducting wall of finite thickness t_c [Eqs. (36–38)]. The conducting wall is coated from inside by a dielectric of thickness t_d. We also obtained the electromagnetic fields excited by an off-axis motion of a point source.

In Fig. 2, the transmission coefficient τ [Eq. (38)] has been visualized as a function of the conducting wall thickness normalized to the skin depth t_c/δ_s, where $\delta_s = \sqrt{(2/\mu_0 S\omega)}$. As in Fig. 2, Fig. 3 shows the transmission coefficient τ as a function of t_c/δ_s using logarithmic scale. Representative machine parameters used in the numerical estimations in Figs. 2 and 3 are: circumference L = 125 m, pipe radius b = 10 cm, beam radius a = 5 cm, dielectric layer with t_d = 3 μm and κ_d = 6, injection energy γ_0 = 1.02, harmonic number n = 5, reference frequency $\omega_0 = \beta_0 c/R$ = 2.41 x 10^6 rad/s, $\omega = n\omega_0$, wall conductivity S = 1.1 x 10^6 $(\Omega\ m)^{-1}$ and δ_s = 0.31 mm.

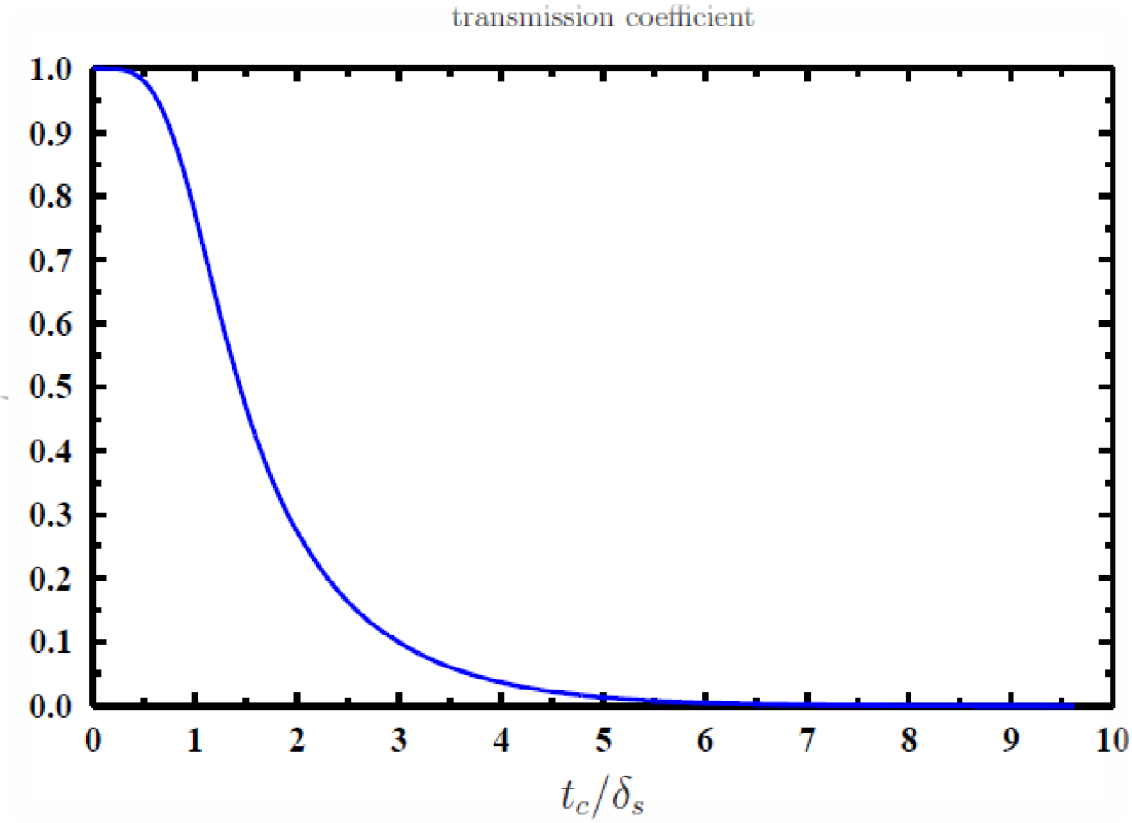

FIG. 2. Transmission coefficient τ as a function of the conducting wall thickness t_c/δ_s. The parameters used are: circumference L = 125 m, pipe radius b = 10 cm, beam radius a = 5 cm, dielectric thickness t_d = 3 μm and κ_d = 6, injection energy γ_0 = 1.02, harmonic number n = 5 and reference frequency $\omega_0 = 2.41 \times 10^6$ rad/s.

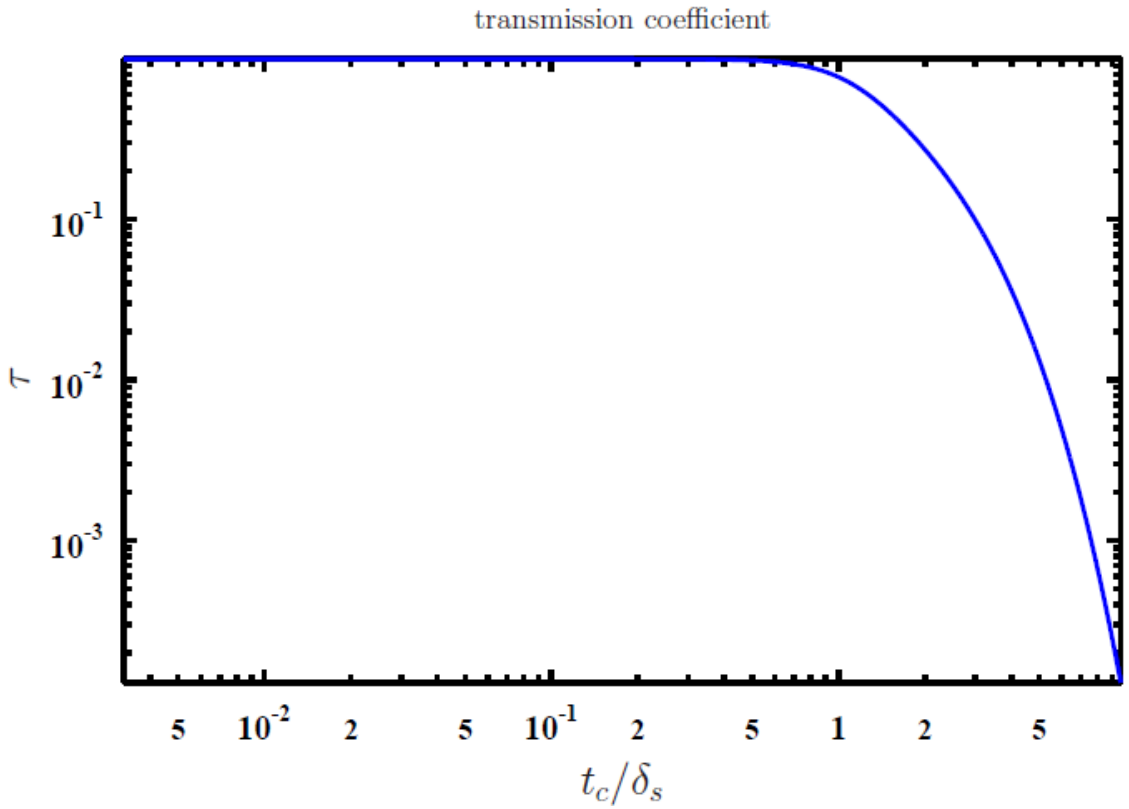

FIG. 3. Transmission coefficient τ (log scale) as a function of the normalized conducting wall thickness t_c/δ_s. The parameters used are: circumference L = 125 m, pipe radius b = 10 cm, beam radius a = 5 cm, dielectric thickness t_d = 3 μm and κ_d = 6, injection energy γ_0 = 1.02, harmonic number n = 5 and reference frequency ω_0 = 2.41 × 10^6 rad/s.

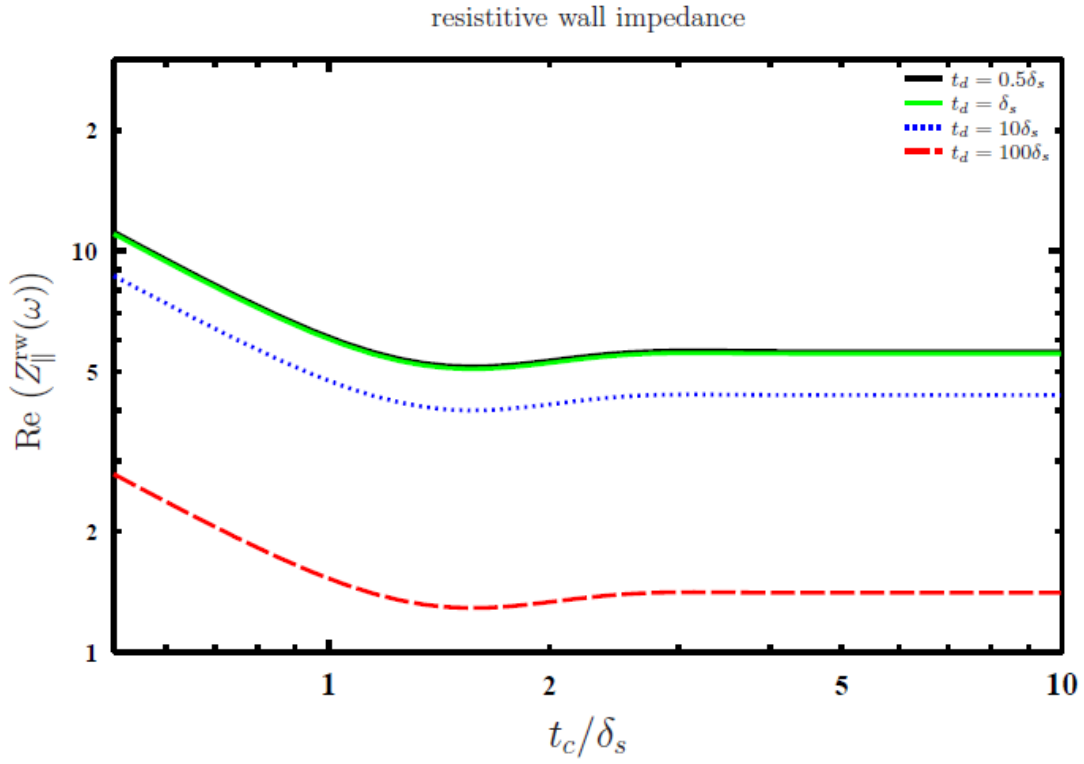

FIG. 4. Real part of the resisitive-wall impedance in Ω as a function of the conducting wall thickness t_c/δ_s. The parameters used are: circumference L = 125 m, pipe radius b = 10 cm, beam radius a = 5 cm, dielectric constant κ = 6, injection energy γ_0 = 1.02, harmonic number n = 5 and reference frequency ω_0 = 2.41 × 10^6 rad/s.

As can be seen in Figs. 2 and 3, the pipe wall is transparent at wall thicknesses t_c less than the skin depth δ_s. At $t_c = \delta_s$, about 0.77% of the incident field penetrates the pipe. By increasing the wall thickness, we observe that only 0.25 % of the incident field can penetrate at $t_c = 2\delta_s$. For standard operation, less than one percent of the field penetrates for $t_c > 5\delta_s$ and field penetration becomes vanishingly small in the thick wall limit. This numerical example shows the importance of the shielding issue in the design of accelerators. Detailed knowledge of the accelerator environment and detailed beam parameters are important in determining the required wall thicknesses needed to shield the wall effectively in order to reduce noise and pipe heating.

Fig. 4 shows, in log-scale, the real part of the resistive–wall impedance of Eq. (37) measured in Ohms as a function of the conducting wall thickness normalized to the skin depth; namely, t_c/δ_s. By varying the dielectric thickness t_d, we observe a suppression in resistive-wall impedance with increasing t_d. As expected, the thick wall limit is reached for $t_c > \delta_s$.

Conclusion

Very good shielding of electromagnetic fields can be achieved by thin metallic walls of thicknesses of the order of few skin penetration depths. Exact field matching has been used to calculate the excited electromagnetic fields and the corresponding longitudinal electric impedance and transmission coefficient. The derived analytical expressions for resistive–wall impedance and transmission have been numerically visualized for some relevant parameters. The validity of the analytical expressions presented in this work is restricted to thin-ring particle beams with a jump discontinuity at $r = a$. In future work, different beam-pipe geometries can be used to investigate impedance and transmission for other beam distributions (RF sources).

The effect of the dielectric thickness t_d on the transmission coefficient is found to be negligibly small, while it leads to a suppression of the resistive-wall impedance for large values of t_d [see Fig.3]. From many numerical runs, we also observed a weak dependance on the dielectric constant κ_d; a result which is already reported in literature [15]. In numerically investigating impedances of multi-layered pipes, the analytical results presented in this work for transmission coefficient and resistive-wall impedance will hopefully be useful in benchmarking numerical codes.

References

[1] Al-Khateeb, A.M., Boine-Frankenheim, O., Hofmann, I. and Ru-molo, G., Phys. Rev. E, 63 (2001) 026503.

[2] Al-Khateeb, A.M., Boine-Frankenheim, O., Hasse, R.W. and Hofmann, I., Phys. Rev. E, 71 (2005) 026501.

[3] Schelkunoff, A., "Electromagnetic Waves", 2nd ed., (D. Van Nostrand Company, Inc, 1943).

[4] Krinski, S., Podobedov, B. and Gluckstern, R.L., Phys. Rev. ST Accel. Beams, 7 (2004) 114401.

[5] Metral, E., Zotter, B. and Slavant, B., IEEE Particle Accelerator Conference, June (2007), p.4216, ISSN 1944-4680.

[6] Hahn, H., Phys. Rev. ST Accel. Beams, 13 (2010) 012002.

[7] Zhilichev, Y., IEEE Trans. Supercond., 23 (2013) 8201810.

[8] Biancacci, N. et al., Phys. Rev. ST Accel. Beams, 17 (2014) 021001.

[9] Cherenkov, P.A., Doklady Akademii Nauk SSSR. 2: 451. Reprinted in Selected Papers of Soviet Physicists, Usp. Fiz. Nauka, 93 (1967) 385.

[10] Sbornike, V. et al., Nauka, (1999), p. 149-153. (Ref. Archived October 22, 2007, at the Wayback Machine).

[11] Genevet, P., Wintz, D., Ambrosio, A., She, A., Blanchard, R. and Capasso, F., Nature Nanotechnology, 10 (2015) 804809.

[12] Jackson, J.D., "Classical Electrodynamics", 3rd ed., (Wiley, New York, 1998).

[13] Collin, R.E., "Foundations of Microwave Engineering", 2nd ed., (McGraw - Hill, N. Y., 1992) pp.108–111.

[14] Pozar, D.M., "Microwave Engineering", Ch. 5, (Addison - Wesley, 1990).

[15] Wang, T.-S. F. and Kurennoy, S., Phys. Rev. STAB, 4 (2001) 104201.